PAPER • **OPEN ACCESS**

Data-driven trajectory optimization in robotic fruit harvesting via deep learning-based perception, gripper configuration, and fruit morphometrics

To cite this article: Sadaf Zeeshan *et al* 2025 *Eng. Res. Express* **7** 045210

Engineering Research Express

OPEN ACCESS

RECEIVED
1 July 2025

REVISED
18 September 2025

ACCEPTED FOR PUBLICATION
30 September 2025

PUBLISHED
10 October 2025

PAPER

Data-driven trajectory optimization in robotic fruit harvesting via deep learning-based perception, gripper configuration, and fruit morphometrics

Sadaf Zeeshan[1], **Muhammad Ali Ijaz Malik**[2,*], **Tauseef Aized**[3], **Akbar Ali**[1], **Simran Ejaz**[1] and **Faiza Javaid**[1]

[1] Department of Mechanical Engineering, University of Central Punjab, Lahore, Pakistan
[2] School of Civil and Environmental Engineering, Faculty of Engineering and Information Technology, University of Technology Sydney, NSW 2007, Australia
[3] Department of Mechanical Engineering, University of Engineering and Technology, Lahore, Pakistan
* Author to whom any correspondence should be addressed.

E-mail: muhammadaliijaz.malik@student.uts.edu.au

Keywords: robotic harvesting, actuation systems, precision agriculture, trajectory optimization

Abstract

Conventional trajectory planning methods for robotic fruit harvesting mainly rely on static geometric heuristics and often overlook critical sensory and task-specific variables such as fruit morphology and end-effector compatibility. These limitations make traditional approaches less effective in real-world agricultural settings, where conditions are unpredictable and fruits require careful, adaptive handling. Moreover, most existing studies do not incorporate a Convolutional Neural Network (CNN) to detect confidence in the planning process, often treating perception and motion planning as isolated components rather than a unified system. To overcome these challenges, this study proposes a data-driven approach to trajectory optimization that integrates visual perception based on CNN confidence levels, gripper type with different actuation technologies, and fruit orientation, parameters that significantly influence harvesting efficiency. Two multivariate regression models were developed, one specifically for firm fruits such as oranges and the other for soft fruits such as strawberries. The models predict trajectory length using three input variables: CNN detection confidence, actuator type, which includes three-finger and two-finger grippers, and fruit orientation angles ranging from 50°–130°. The non-linear influence of orientation is captured through polynomial terms. A total of 46 experimental trials were conducted for each fruit type using a robotic platform under controlled conditions. The regression outputs revealed that CNN confidence had a strong influence on trajectory length reduction, while orientation had a more severe impact on strawberries due to their delicate structure. In comparison to baseline trajectories, the optimized A* planner, guided by regression coefficients, curtailed trajectory lengths by 11% for strawberries and 14% for oranges. Moreover, the positional accuracy incre ased by 15% and 12%, respectively. The higher predictive accuracy was attained by the models (R^2 = 0.89 and 0.82; RMSE = 3.2 cm and 4.7 cm for strawberries and oranges, respectively). These results demonstrate that heuristic planning, combined with statistical modeling, enhances motion reliability and spatial efficiency in autonomous fruit picking.

Nomenclature

AP	Average Precision
CBAM	Convolutional Block Attention Module
CMMD	Central Moment Discrepancy
CNN	Convolutional neural network

DC motors	Direct Current Motors
DOF	Degrees of Freedom
3D	Three-dimensional
EDGC	Edge-Directed Grid Constrained
FID	Fréchet Inception Distance
FPS	Frames Per Second
LED	Light-emitting diode
RRT	Rapidly Exploring Random Tree
MAPE	Mean absolute percentage error
MARTA	Multi-Agent Real-Time Architecture
mIOU	Mean Intersection over Union
PRM	Probabilistic Roadmap
TL	Trajectory length
R^2	Coefficient of determination
RMSE	Root mean square error
RGB-D	Red Green Blue—Depth
SSD	Solid state drive
YOLO	You Only Look Once

Introduction

The global agricultural sector is certainly going through a transitional phase, determined by the cumulative requirement for sustainable food production through conventional labor-intensive farming practices [1]. The higher labor costs and a growing scarcity of agricultural land serve as two critical factors in food insecurity [2]. The cost associated with agricultural production has been significantly augmented in developing nations, especially in the subcontinental region like Pakistan, which ranged from 12.6 to 30% between 2023 and 2024 [3]. Likewise, this escalating inflation, upsurging rural-to-urban migration, and lack of technological agricultural advancements have resulted in a severe upsurge in agricultural labour costs [4]. The lack of technological advancements in the agricultural sector is a major challenge in the evolution of the sector [5]. It has been estimated that around a 30 to 40% reduction in operational costs can be achieved through robotic fruit harvesting practices [6]. Moreover, the automated harvesting systems result in improved yield quality, higher productivity, and lower operational costs [7]. However, current fruit-picking systems continue to perform below optimal levels despite significant developments in agricultural robotics, especially in unstructured contexts with occlusions, variable lighting, and variable agricultural production rates [8]. The conventional trajectory planning systems faced limitations in sensory feedback [9], fruit morphology [10], and the dynamic interaction between robotic end-effectors and the target [11]. The trajectory planning is essential to current agricultural robots because it guarantees both the fruit's reachability and the effectiveness of the gripping and detaching operation [12]. By avoiding static impediments, conventional trajectory-planning frameworks like geometric models, heuristic techniques, or sampling-based planners like Dijkstra, A*, RRT, and PRM are suitable for navigating structured environments. However, combining precise fruit detection with gripper-aware planning can greatly increase their efficacy. Conventional approaches tend to isolate perception from actuation and frequently presume that the fruit and its environment are both rigid and unchanging. Their capacity to handle problems in the real environment, like asymmetrical fruit orientations, occlusions from leaves and branches, and changes in size, shape, or softness, is hampered by this separation.

The fruits should be selected during a brief window of maturity, when their quality is at its peak. When the strawberries achieve the proper sweetness and turn completely red, they are often plucked in the spring or early summer [13]. In contrast, oranges are usually picked in the colder winter months based on the color of the peel and the balance of sugar and acid [14]. To guarantee the best quality and output, robots must be used to pick fruits exactly within the designated season. Harvest time and success rate are critical performance indicators in robotic fruit harvesting. Previous research has shown that robotic systems can achieve promising success rates, with harvesting times getting close to realistic levels for field application. The current research practices show promising advancements in robotic fruit harvesting for oranges and strawberries. Harvest durations for strawberries are usually between 4 and 11 s per fruit, and success rates have been continuously increasing, ranging

Table 1. Recent advancements in success rates and harvest times through robotic harvesting of strawberries and oranges.

References	Year	Fruit	Harvest time	Success rate
Luis *et al* [15]	2024	Strawberries	7.5s	71.7%
Yu *et al* [16]	2024	Strawberries	4.7–7.3 s	—
Xie *et al* [17]	2025	Strawberries	4.5 s	87.2%
He *et al* [18]	2025	Strawberries	10.9s	91.4%
Yin *et al* [19]	2023	Oranges	10.9s	87.2%
Zeeshan *et al* [20]	2024	Oranges	7.2s	90.5%
Xiao *et al* [21]	2024	Oranges	—	87.15%

from about 72% to over 91% [15–18]. Oranges exhibit a comparable pattern, with picking times averaging 7–11 s and success rates continuously between 87%–90% [19–21]. It shows that fruit harvesting robots are attaining reliability in the identification and harvesting of fruit in practical situations. Table 1 summarizes the reported success rates and harvest times through automated agricultural practices.

A successful robotic grip can be achieved through an optimal approach angle and by applying the appropriate contact forces when accurate fruit localization and appropriate physical characterization are integrated. At the same time, trajectory planning that considers the gripping mechanism's constraints and design guarantees that the movement is both collision-free and optimized for a steady and effective pick. The integration approach results in trajectories that maximize the probability of successful harvesting, decrease trajectory length and energy consumption, and eliminate needless reorientations. The planning process becomes more intelligent and context-aware when perception and gripping restrictions are considered together. This produces better results than traditional and detached approaches. An effective substitute for rule-based trajectory planning in robotic decision-making is the incorporation of data-driven approaches. The robots can learn task-specific patterns from data and interpret complicated visual signals with high accuracy by utilizing machine learning, especially deep learning models like Convolutional Neural Networks (CNNs). The challenges involving the identification and categorization of fruit, CNNs have shown remarkable performance [22–29]. The fruits can also be detected through the application of YOLO models [30–35]. However, their output confidence scores remain underutilized in downstream motion planning processes. These confidence scores, when interpreted as a proxy for perceptual certainty, can be invaluable in guiding more informed and adaptive trajectory generation. Moreover, the mechanical interface between the robot and the fruit and the end-effector plays a pivotal role in determining the feasibility and efficiency of the trajectory executed. Different fruit types require different handling strategies: firm fruits, such as oranges, may be better suited for rigid three-finger grippers [36], while delicate fruits like strawberries often necessitate a compliant, two-finger [37] or suction-based actuators. To date, the interplay between visual perception, gripper configuration, and fruit morphology has been insufficiently explored in the context of trajectory optimization. Most existing studies treat these components in isolation, leading to suboptimal performance in real-world deployments. For instance, Vrochidou *et al* [38] provided an early overview of robotic harvesting systems but noted the critical challenge of end-effector adaptation. Lehnert *et al* [39] developed autonomous systems for capsicum harvesting, incorporating perception and motion planning, but their methods did not dynamically adjust trajectory planning based on actuator type or fruit pose. Similarly, Zu *et al* [40] and Sa *et al* [41] focused primarily on improving fruit detection and segmentation using CNNs without leveraging this perception data for motion trajectory optimization.

Many models for agricultural produce detection have been tested. Wang, F [42] achieved accurate wheat spike segmentation using an adaptive k-means algorithm and estimated spike volume through cuboid fitting. Bai *et al* [43] proposed a hybrid U-Net + YOLO-v3 model that achieved superior cucumber detection with an AP of up to 99% and mIOU of 94.24%, outperforming standalone models. The fused approach improved feature extraction, enhancing prediction accuracy by 6%. This method proved robust for fruit detection in complex environments and supports automated harvesting and yield estimation. Roggiolani *et al* [44] proposed a method that generated realistic 3D leaf point clouds conditioned on specific traits (length and width), outperforming other synthetic datasets like Helios and LiDiff in terms of Fréchet Inception Distance (FID), F-score, and CMMD across multiple plant species. Tuning leaf trait estimation models on the generated data significantly improved the accuracy of leaf length and width predictions. The generated leaves closely matched real-world distributions and provided per-leaf ground truth, enabling finer, more reliable trait analysis. Singh *et al* [45] used OLOv9-GLEAN model to achieve high strawberry detection accuracy, with a precision of 0.996 and recall of 0.991. Trained on both real and synthetic images, it showed strong adaptability across diverse datasets. The model was validated in a ROS-Gazebo digital twin of the SILAL greenhouse and integrated with the MARTA robot, enabling precise visual servoing and effective strawberry grasping. Zhang *et al* [46] found that the EDGC-YOLO model significantly improved green citrus detection by optimizing anchor box

generation using aspect ratio analysis and BGMM adjustment. With Refined-EfficientNetV2 and CBAM integration, the model reduced parameters to 4.52M and size to 9.4 MB, while achieving increases of 0.5% in precision, 1.6% in recall, and 3.0% in mAP. This lightweight, high-accuracy model supports real-time decision-making for green citrus harvesting robots. Kaleem *et al* [47] addressed the high data consumption problem in deep learning-based pest control by proposing an Edge Distance-Entropy data evaluation method. The method reduced data usage by 5% to 15% compared to existing approaches and achieves 100% effectiveness using only 60% of the data. Experimental results confirmed that it outperformed other evaluation methods, offering a more efficient solution for crop pest detection. This contributed significantly to the sustainable development of smart agriculture by reducing resource dependency. Miao *et al* [48] developed an advanced tomato-harvesting robot by integrating traditional image processing with the YOLOv5 deep learning model to improve crop and stem recognition in complex agricultural environments. An algorithm was proposed to estimate truss tomato maturity and accurately locate stems, and the robot achieved efficient harvesting performance for the tomato cluster. Researchers have also found that the gripper affects fruit harvesting efficiency. Navas *et al* [49]. analyzed the grippers used in the harvesting process and suggested soft grippers as the most promising technology for agricultural harvest. Elfferich *et al* [50] suggested soft grippers had the most successful rate in fruit harvesting. Visentin *et al* [51] explored that different fruits require different gripper forces. Delicate strawberries require sophisticated, soft grippers, unlike stiff, classical grippers.

In recent work, researchers have begun exploring the benefits of coupling machine vision with actuator control. For example, Kurtser *et al* [52] researched on robotic perception to adapt robotic arm movement in real time. However, even these systems seldom incorporate quantitative models that link CNN detection confidence, fruit pose, and actuator characteristics to motion planning parameters such as trajectory length or trajectory smoothness. This disconnect limits the robot's capacity to make context-aware decisions during the harvesting task. Addressing this gap, the present study proposes a novel data-driven framework for trajectory optimization in robotic fruit harvesting, which explicitly models the relationship between deep learning-based perception (CNN confidence), actuator type, and fruit morphometrics (especially orientation angles). The core hypothesis is that by capturing these relationships through regression-based learning models, robots can predict and execute more efficient motion trajectories that are tailored to both the fruit type and the interaction dynamics of the gripper. To empirically validate this framework, two multivariate regression models were developed: one for firm fruit, oranges, and another for soft fruit, strawberries. Each model takes as input (1) the CNN confidence score reflecting detection certainty, (2) the type of gripper (three-finger or two-finger), and (3) the fruit's orientation angle within a defined range (50°–130°). Notably, the model captures the non-linear influence of orientation through polynomial terms, acknowledging that the angle at which fruit is presented significantly affects the trajectory required for successful harvesting. The current study makes several key contributions to the field of precision agriculture and agricultural robotics:

- It introduces systematic integration of deep learning-based perception and mechanical actuation parameters into trajectory planning, addressing the fragmented nature of prior approaches.
- It establishes a quantitative link between CNN confidence, gripper configuration, and fruit pose, enabling context-aware trajectory optimization.
- It presents empirical evidence demonstrating the effectiveness of data-driven trajectory models in reducing trajectory length, which directly impacts efficiency and task throughput.

By unifying perception, actuation, and motion planning under a data-driven umbrella, this research lays the groundwork for more autonomous, adaptive, and efficient harvesting systems. The proposed framework moves beyond traditional, siloed paradigms and represents a significant step toward intelligent robotic systems capable of operating in the dynamic and uncertain environments of modern agriculture. The Introduction section presents a comprehensive overview of the research, along with a critical review of relevant literature to establish the research gap. The Materials and Methods section defines the empirical approach, constituting the system design, deployment scenarios, and the selected parameters. The Results and Discussion section portrays a comprehensive set of experimental findings, detailing their significance and implications for optimal robotic trajectory planning performance. Finally, the Conclusion section recaps the significant findings through scientific relevance and proposes future recommendations.

Material and methods

Methodology

The multivariate linear regression models were developed and validated through a data-driven methodology to forecast the ideal trajectory length (P) for fruit harvesting robots. The CNN-based detection confidence score (C), which was derived from fruit recognition using an RGB-D Kinect v2 camera, the gripper type (G), which was represented by one-hot encoding to differentiate between two-finger and three-finger silicon grippers, and the fruit orientation (O), which was measured as angular displacement (50°, 70°, 90°, 110°, 130°) relative to the vertical axis, representing grasping approach angles, were the three main independent variables that were incorporated into the models. Image data captured from the RGB-D Kinect v2 camera was processed using a convolutional neural network (CNN), which generated real-time detection confidence values. These were combined with experimental data on gripper type and fruit orientation to construct the regression input dataset. Separate models were trained for firm fruits (oranges) and soft fruits (strawberries), each comprising 46 trials to capture their respective physical handling characteristics. The robotic platform was based on a 5-DOF arm designed by Zeeshan *et al* [20], upgraded for enhanced control and data acquisition. A closed-loop feedback control system was implemented using DC motors equipped with rotary encoders, enabling precise joint actuation and real-time position feedback. The encoder data were processed via a Raspberry Pi 4 microcontroller, which managed control signals and interfaced with motor driver modules (L298N) to actuate the robotic joints. The control logic facilitated accurate trajectory tracking and gripper alignment, whereas the Kinect camera simultaneously provided depth and color data for target localization and distance estimation. The regression models were evaluated using the coefficient of determination (R^2), Root Mean Square Error (RMSE), and Mean Absolute Percentage Error (MAPE). This statistically informed model was then translated into a real-time cost function, which was embedded into the A^* algorithm to guide the robot's trajectory planning. To influence the cost function f(n), the expected trajectory length (T) was incorporated into an A^* trajectory planning algorithm. With constant feedback from the Kinect and encoder data, this system allowed for dynamic trajectory optimization based on real-time perception and grasp configuration. The system, which is built for two different monoculture deployments, has a local trajectory planning architecture that enables it to adjust in real time to variables like gripper alignment, CNN detection confidence, and fruit position. For both fruit varieties, the device successfully replicated actual harvesting conditions in a controlled laboratory environment.

Design and experimental set-up

Experiments carried out in regulated lab settings confirm the data-driven regression-based approach for trajectory planning optimization in a robotic fruit harvesting system. The robotic platform with a 5-DOF articulated manipulator is given in figure 1. The articulated manipulator with silicon grippers and all the linkages is seen in figure 1(a). The manufactured robot is depicted in figure 1(b). Fruit detection and localization depend on the color and depth information provided by the RGB-D sensor in the frame. Real-time fruit type identification and classification is achieved using a convolutional neural network (CNN)-based vision system, which allows for adaptive decision-making for trajectory planning and grasp execution. The current study presents a data-driven regression-based framework for optimizing trajectory planning in a robotic fruit harvesting system, validated with experiments conducted under precisely controlled laboratory conditions. Figure 1 shows the robotic platform consisting of a 5-degree-of-freedom (DOF) articulated manipulator. Figure 1(a) shows the articulated manipulator with silicon grippers, with all the links. Figure 1 (b) shows the fabricated robot. The RGB-D sensor on the frame provides both color and depth information essential for fruit detection and localization. A convolutional neural network (CNN)-based perception system is implemented to identify and classify fruit types in real-time, enabling adaptive decision-making for grasp execution and trajectory planning.

The experimental setup was designed to evaluate performance across two fruit categories, firm (oranges) and soft (strawberries), representing distinct tactile and geometric characteristics. To accommodate variations in fruit morphology and compliance, the end-effector of the robot was configured with interchangeable silicon grippers of two types: 2-finger and 3-finger designs. Multiple grasp orientations and approach angles were tested for each gripper-fruit combination to assess their influence on motion smoothness, grasp stability, and trajectory planning efficiency. Figure 2 shows the grippers used for the experiment. Figure 2(a) shows the silicon gripper with two fingers, and figure 2(b) shows the silicon gripper with three fingers.

The robotic arm operated within a defined planar workspace of 0.7×0.7 m, positioned on a vibration-damped, matte-finished laborat ory surface to eliminate visual artifacts. All experiments were conducted under ambient environmental conditions maintained at 26 ± 1 °C temperature and approximately 50% relative humidity. The environmental settings were selected to reflect typical orchard conditions while ensuring

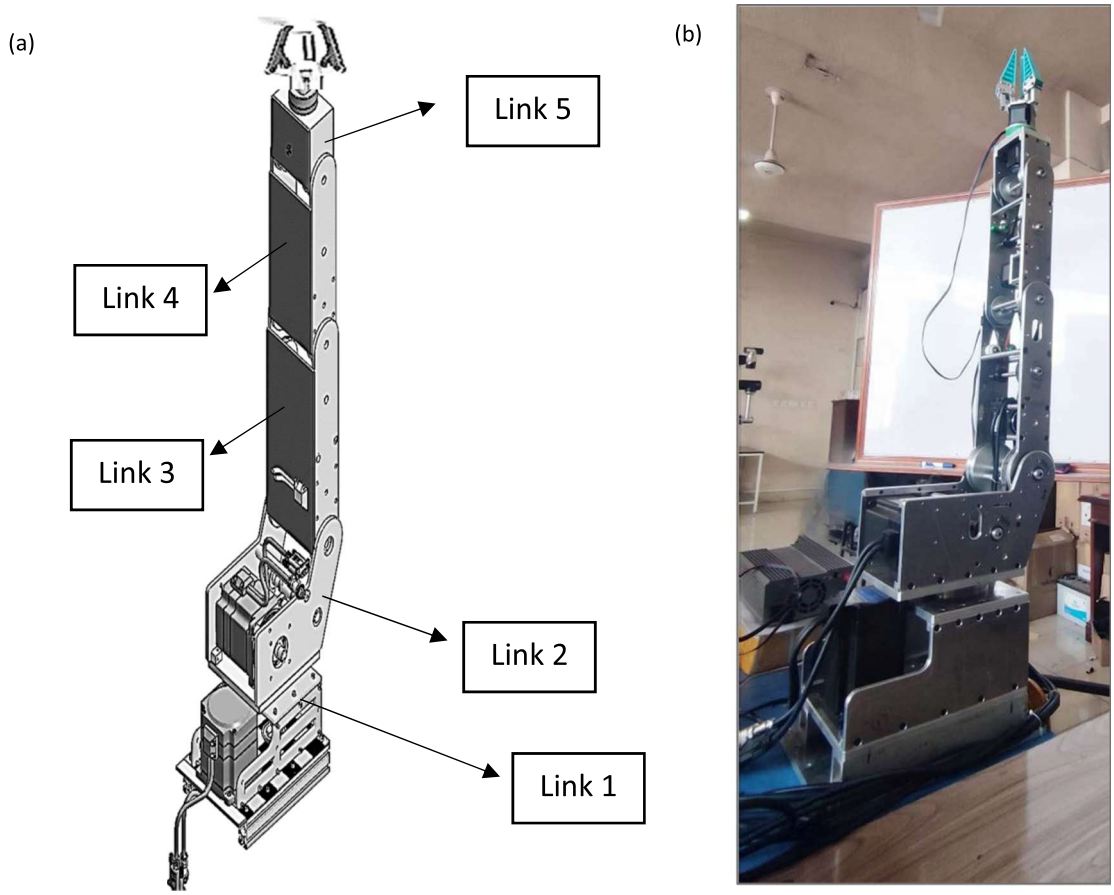

Figure 1. Five-degree-of-freedom (DOF) articulated manipulator with the silicon grippers: (a) illustrations of all links, and (b) illustrations of the fabricated robot.

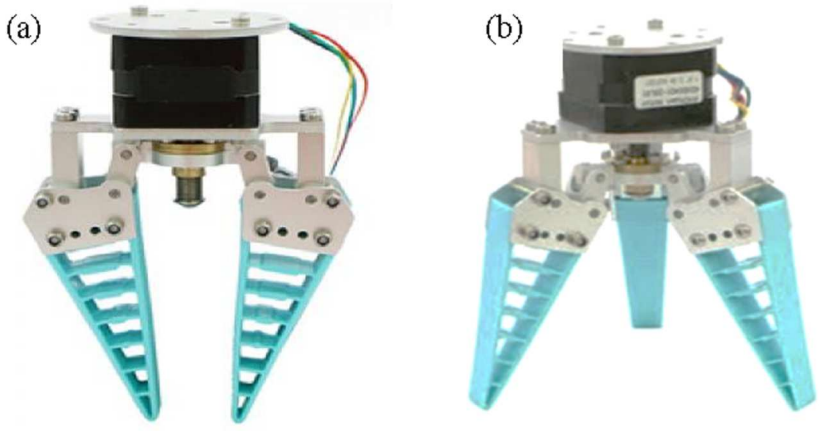

Figure 2. Silicon grippers: (a) two-finger, and (b) three-finger.

consistency in sensing and manipulation. The air temperature was maintained at 26 °C, which is commonly observed during harvesting hours and helps preserve both fruit firmness and the performance of the gripper material. Light levels were kept around 1000 lux, similar to shaded-canopy or bright-overcast conditions. Relative humidity was controlled at 50%, a moderate value often present in orchards, chosen to avoid condensation on the fruit and sensors while also preventing fruit drying. Together, these parameters provided conditions that were both realistic and standardized for the strawberry and orange trials. Lighting was controlled using daylight-balanced light-emitting diode (LED) arrays to maintain a constant illumination level of 1000 lux, ensuring consistent image acquisition and eliminating illumination-based noise in perception tasks. To support robust fruit classification, a custom dataset comprising 1500 annotated RGB-D images was generated from

multiple real-world trials under varied orientations and lighting perspectives. The dataset included equal representation of both target fruits and incorporated images across different grasping angles and distances. The data were labeled using open-source annotation tools and subsequently pre-processed through normalization and augmentation (e.g., random rotations, brightness adjustment) to enhance model generalizability. The dataset was split using a standard 70:30 ratio, allocating 1050 images for training and 450 for validation/testing. The CNN architecture employed was a modified version of MobileNetV2 due to its balance between computational efficiency and accuracy, and was trained using the Adam optimizer with a learning rate of 0.001, batch size of 32, and stopped based on validation loss, having a maximum epoch of 70.

The entire perception and planning pipeline was executed on a Dell Inspiron 11th-generation laptop equipped with an Intel Core i7 processor, 8 GB RAM, and a 512 GB solid-state drive (SSD), operating on Windows 10 (64-bit). A multivariate regression model was subsequently developed to correlate the CNN-derived object features (e.g., fruit type, size, centroid coordinates), end-effector configuration, and fruit physical characteristics with robotic motion planning metrics such as total trajectory length, task execution time, and collision occurrences. The model was trained using empirical data collected from repeated harvesting trials and validated by comparing predicted trajectories against actual robot motion. This enabled dynamic trajectory prediction and selection of optimal trajectories based on task-specific and environmental constraints, thereby minimizing redundant movements and enhancing harvesting efficiency. The inclusion of multiple trials for each condition ensured the statistical robustness and repeatability of the proposed framework. The experimental design of this study centers on modeling the influence of three critical parameters, CNN-based visual confidence (C), gripper type (G), and fruit orientation (O), on the optimization of trajectory length (P) in robotic fruit harvesting. A multivariate linear regression approach was adopted to quantify the relationship among these variables, allowing for the development of fruit-specific predictive models. The gripper type, a categorical variable representing commonly used mechanisms in agricultural robotics (3-finger and 2-finger), was encoded using dummy variables. Orientation was treated as a continuous angular variable representing the fruit's axis relative to the robot's end-effector. The proposed regression model takes the general form:

$$Y = \beta_0 + \beta_1 X_1 + \beta_2 X_2 + \beta_3 (X_3 - 90^\circ)^2 + \varepsilon$$

Where β are Regression coefficients while X_1, X_2, and X_3 show CNN confidence score, gripper type, and gripper orientation, respectively. Y is the trajectory planning output and ε is the error term.

Separate models were trained for firm fruits (e.g., oranges) and soft fruits (e.g., strawberries) to account for differing interaction dynamics. These regression outputs were subsequently integrated into the A* trajectory planning algorithm, where predicted trajectory length influenced the cost function *f(n)* thereby enabling dynamic adjustment based on fruit morphology and harvesting constraints. The cost function is given as:

$$f(n) = g(n) + h(n)$$

Here the cost function is the total estimated cost from start to goal via node n, g(n) is the actual cost from start to n, and h(n) is the heuristic estimate from n to the goal. The traditional A* trajectory cost function was modified to incorporate perception and hardware-based parameters,

$$g(n) = d(n) + \alpha(1 - C_{CNN}) + \beta|\theta - \theta_{opt}| + \gamma T_g$$

Here, d(n)is the Euclidean distance to node n, C_{CNN} is the CNN confidence score for fruit detection, θ is the current gripper orientation, θopt is the optimal alignment angle, and Tg denotes a categorical value assigned to the gripper type. The weights α, β, γ were empirically determined to balance the influence of each parameter. This approach enabled the trajectory planner to favor trajectories that not only minimize travel distance but also optimize perception reliability and grasping feasibility, resulting in shorter trajectories and improved positional accuracy during fruit acquisition.

Deployment environment

The system is designed for deployment in semi-structured agricultural environments, such as small-scale orchards or indoor greenhouses, with known map layouts. For strawberry harvesting, deployment conditions should be in a controlled indoor greenhouse environment characterized by flat terrain and structured planting rows. The inter-row spacing ranged between 0.8–1.0 meters should be there for easy robot manoeuvrability. Lighting conditions range between 1000–1500 lux, sufficient for CNN-based visual detection. Obstacle heights (such as bed edges or irrigation lines) to be limited to 0.2–0.4 meters, allowing for safe navigation. The environment should be static during the harvesting phase, with minimal variation in ambient conditions. For orange harvesting, the robot deployment conditions are for small-scale orchard blocks, characterized by natural daylight ranging between 8000–10000 lux. Tree canopies with a height range from 2.5 to 3.5 meters, and the inter-row spacing of 2.5–3.0 meters, are allowed for sufficient clearance for the robotic platform to traverse and align with target fruit. The terrain is mostly flat and dry, with minor surface irregularities.

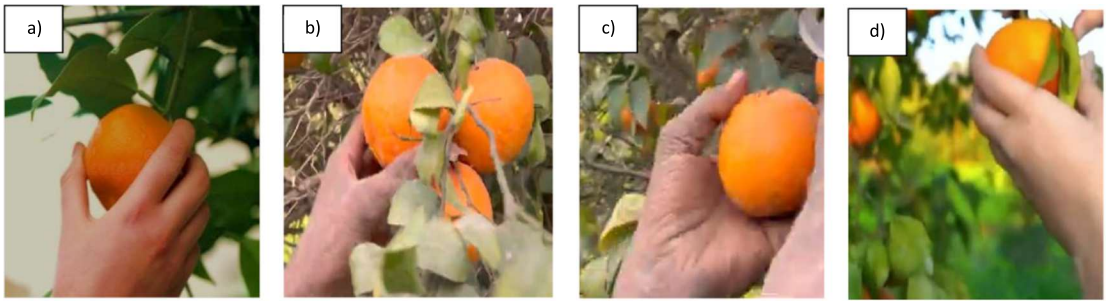

Figure 3. Varying gripping angles for picking Orange fruit: (a) grip at 90°, (b) grip at 110°, (c) grip at 80°, and (d) grip at 70°.

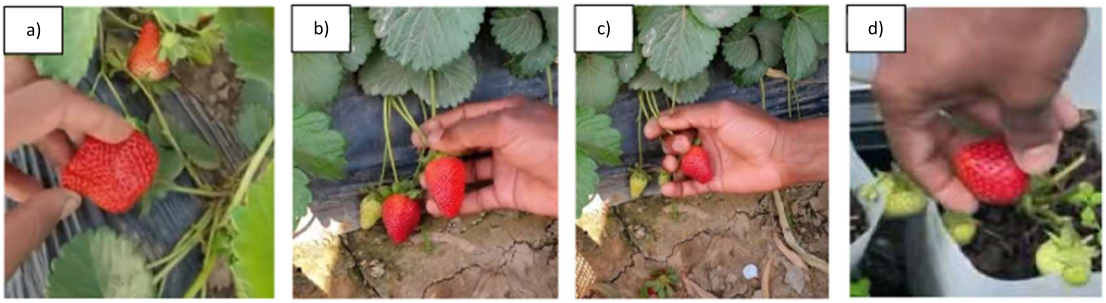

Figure 4. Varying gripping methods for picking Strawberry fruit: (a) grip at 90°, (b) grip by stem pull, (c) grip by stem break, and (d) grip at an angle.

In both deployments, the robot is designed to operate under a local trajectory planning scheme, continuously adapting in real-time to fruit pose, CNN detection confidence, and gripper positioning. The current system is designed for monoculture operations, where a single crop type is handled per deployment. Nevertheless, the architecture is modular and scalable, and in future studies, it can be extended to support global planning strategies, such as coordinated multi-row traversal or crop switching, through the integration of higher-level task allocation and map-based planning layers. The system performs reliably using mid-range computational hardware (Intel Core i7 @ 2.30 GHz, 16 GB RAM, GPU with 6 GB VRAM). The deployed system incorporates low-latency processing, enabling real-time inference and trajectory updates with a cycle time of 100–150 milliseconds to ensure responsive action. An integrated RGB-D camera allows the system to perceive the 3D structure of the environment, including branches, fruits, and other potential obstacles. By utilizing the depth map, the system effectively identifies and localizes obstacles within the robot's path, facilitating the computation of a collision-free trajectory in real time. These specifications support real-time vision and motion planning without requiring high-end infrastructure. Thus, under the stated monotype and semi-structured deployment conditions, the overall cost remains manageable, promoting the feasibility of commercial-scale application.

Gripping angle

The gripping angle is a critical parameter in robotic fruit harvesting, as it directly affects the stability, effectiveness, and safety of the grasp, particularly when handling fruits with diverse mechanical properties. Hard fruits like oranges, which exhibit higher structural rigidity and peel toughness, can typically withstand greater gripping forces, up to approximately 80 N, without risk of surface damage or deformation. This mechanical resilience allows for a wider range of permissible gripping angles and firmer end-effector contact, enhancing positional tolerance during grasping. Figure 3 shows various gripping angles for picking oranges, such as the grip at 90° (see figure 3(a)), grip at 110° (see figure 3(b)), grip at 80° (see figure 3(c)), and grip at 70° (see figure 3(d)). In contrast, soft fruits such as strawberries possess delicate skin and low compressive strength, necessitating much lower gripping forces, typically in the range of 8–12 N, to prevent bruising, tearing, or tissue collapse. Figure 4 shows various gripping angles for picking strawberries, such as the grip at 90° (see figure 4(a)), grip by stem pull (see figure 4(b)), grip by stem break (see figure 4(c)), and grip at an angle of 110° (see figure 4(d)). The field observations confirm that the most effective techniques for harvesting oranges and strawberries involve either grasping the fruit at an angle of approximately 90° or within the 70–100° range or

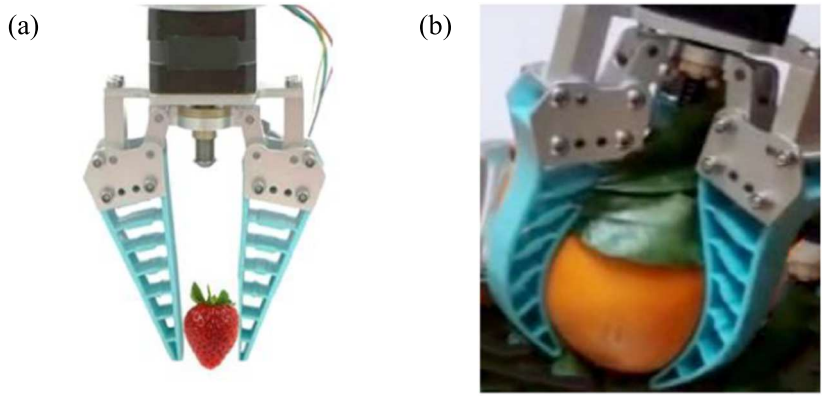

Figure 5. (a) Two-finger silicon gripper for Strawberry fruit picking, and (b) Three-finger silicon gripper for Orange fruit picking.

alternatively detaching the fruit by cutting the stem. These approaches are consistent with natural hand-picking practices, where such angles provide optimal leverage to detach the fruit while minimizing mechanical stress and surface damage. The findings were obtained through direct observation of skilled farm workers during harvest in local farms, highlighting the practical relevance of these methods for designing robotic grippers that can replicate safe and efficient picking.

The approach angle of the gripper determines the distribution of contact forces and the extent of surface engagement, which are especially critical for soft produce. A non-optimized angle can result in localized pressure points, shear forces, or incomplete contact, leading to unsuccessful picking attempts or post-harvest quality degradation. For strawberries, a nearly perpendicular approach with a compliant grasping mechanism is often required to distribute forces uniformly and reduce peak contact pressure. Conversely, for oranges, angular flexibility allows for side or angled approaches without compromising structural integrity. Therefore, optimizing the gripping angle is also fruit-specific and hence, is dynamically adaptable, integrating the knowledge of fruit morphology, surface compliance, and mechanical limits to achieve high grasp success rates while maintaining fruit quality.

Gripper type

In robotic harvesting applications, the selection of the right end-effector is critical for ensuring both grasp stability and produce integrity. This study used two types of soft, compliant silicone grippers, a 2-finger and a 3-finger configuration, selected for their mechanical adaptability to different fruit morphologies and textural properties. The 2-finger gripper, with its reduced contact surface and lower gripping force range (8–12 N), is well-suited for soft fruits such as strawberries, causing minimal pressure distribution to prevent epidermal bruising and internal tissue deformation or damage. A two-finger silicone gripper, unlike a three-finger design, minimizes the overall contact area with delicate fruits such as strawberries, which are highly susceptible to bruising. By limiting the contact points along with applying carefully controlled force, the two-finger configuration reduces pressure concentration and ensures a gentler, safer grip on small, fragile fruits. Furthermore, its simpler geometry allows easier access and greater maneuverability within dense fruit clusters, where a three-finger gripper may cause obstruction or accidental compression of adjacent and nearby strawberries. The reduced structural complexity also improves responsiveness and handling, making the two-finger gripper particularly well-suited for safe and efficient harvesting of soft produce like strawberries. In contrast, the 3-finger gripper provides a more geometrically stable, tri-contact configuration that is capable of withstanding higher gripping forces (up to ~ 80 N), making it appropriate for firm fruits like oranges, where structural rigidity allows more aggressive grasping without compromising quality. Figure 5(a) demonstrates fruit gripping by a 2-finger gripper, and figure 5(b) shows the 3-finger gripper gripping an orange without avoiding excess force. These compliant silicone grippers were intentionally selected over suction and metallic grippers due to functional limitations observed in unstructured agricultural environments. Suction grippers often exhibit poor adherence on non-planar, moist, or textured surfaces, conditions commonly encountered with natural fruits, leading to grasping inconsistencies and detachment failures. Metallic grippers, while offering high structural stiffness, lack the compliance necessary to handle biologically soft materials and substantially increase the risk of mechanical damage due to excessive point loading. Silicone grippers, in contrast, offer low modulus elasticity, surface conformance, and inert chemical properties, which collectively enable secure, non-destructive grasping across a spectrum of fruit types and orientations. To further enhance the generalizability and robustness of the trajectory planning model, future testing will incorporate a broader

range of end-effector designs, including adaptive, underactuated, and soft pneumatic grippers, to quantitatively evaluate the impact of gripper mechanics on trajectory optimization, grasp success rates, and task execution efficiency in variable harvesting scenarios.

The current silicone-based gripper design has been experimentally validated for strawberries and oranges, demonstrating effective performance in terms of grasp stability and fruit safety. Given its compliance and adaptive geometry, the gripper may also be suitable for handling fruits with similar physical characteristics, such as plums or tomatoes. However, its universal applicability remains limited, and further experimental testing and parameter tuning are necessary to ensure reliable operation across a broader range of horticultural produce. While the integrated regression model supports the inclusion of alternative gripper configurations through re-encoding of input parameters, the mechanical design must be revalidated for significantly different fruit types, such as grapes or pears. To improve the system's generalizability, future research should investigate modular or interchangeable gripper architectures, including suction-based end-effectors, to accommodate a wider spectrum of fruit morphologies.

CNN-based visual confidence

To support robust fruit classification under variable conditions, a CNN-based visual confidence metric (C) was introduced to quantify the model's certainty in identifying and localizing fruit targets. The confidence score C, ranging from 0 to 1, is derived from the final SoftMax output layer of the CNN and reflects the probability associated with the predicted fruit class. A higher *C*-value shows stronger visual certainty, which is critical in decision-making for grasp execution and trajectory planning, particularly in cluttered or partially occluded environments [53]. The bespoke dataset of 1500 annotated RGB-D photos from actual fruit harvesting attempts was assembled to develop the current model. The different orientations, gripping angles, and distinct lighting conditions (800–1200 lux) were all included in these annotated photos. An equal distribution of oranges and strawberries was included in the dataset, which was labeled using the LabelImg program. To improve generalizability, the dataset was enhanced with methods including random rotations ($\pm 30^{\circ}$), brightness variations ($\pm$20%), and zooming ($\pm$15%).

A 70:30 split was used to divide the dataset, allocating 450 photos for validation and 1050 images for training. Data augmentation methods, such as illumination shifts, rotation, zoom, and occlusion, were used to enhance performance in various lighting scenarios, such as day and night. By adding more variety to the training set, these augmentations improved the model's generalization and decreased the possibility of overfitting. Additionally, by combining RGB and depth information, the system was able to consistently detect fruit even in the presence of changing ambient lighting. The balanced trade-off between accuracy and computing performance on edge devices serves as a prime reason for the selection of a modified MobileNetV2 architecture. The current model was trained using the Adam optimizer with a learning rate of 0.001, having a batch size of 32, and early stopping criteria based on validation loss. Validation accuracy (~92%) remained stable throughout, indicating effective generalization. Cross-entropy loss was used as the objective function. During inference, predictions with $C \geqslant 0.85$ were considered highly reliable and directly used for initiating the grasp sequence, while detections with $C < 0.6$ were flagged for further inspection or re-evaluation from an alternate viewpoint. This confidence-based gating mechanism enabled the robotic system to adaptively decide whether to proceed with grasping or refine its visual perspective, thus enhancing the robustness and safety of fruit harvesting under real-world variability. Figure 6(a) displays the CNN model results for the detection of Oranges, and figure 6(b) shows the CNN model results for the detection of Strawberries after fine-tuning the model. Hyperparameters are displayed in table 2.

Results and discussion

The regression coefficients presented in the trajectory length models for fruit harvesting were obtained through controlled laboratory experiments. In these tests, a robotic harvesting system was deployed to collect data on various scenarios involving different CNN confidence levels, gripper types, and end-effector orientations. The experiments were conducted separately for firm fruits (oranges) and soft fruits (strawberries) to capture their distinct handling requirements. Multiple trials were recorded under varying conditions, and the resulting trajectory lengths were measured. Using this experimental dataset, a multiple regression analysis was performed to determine the quantitative relationship between the input variables and the observed trajectory length, Y.

$$Y\,(oranges) = 51{\cdot}37 - 9{\cdot}67X_1 + 0{\cdot}34X_2 + 0{\cdot}02(X_3 - 90^{\circ})^2 + \varepsilon$$

$$Y\,(strawberries) = 51{\cdot}35 - 6{\cdot}41X_1 + 0{\cdot}25X_2 + 0{\cdot}04(X_3 - 90^{\circ})^2 + \varepsilon$$

where X_1, X_2, and X_3 show CNN confidence score, gripper type, and gripper orientation, and Y is the trajectory planning output.

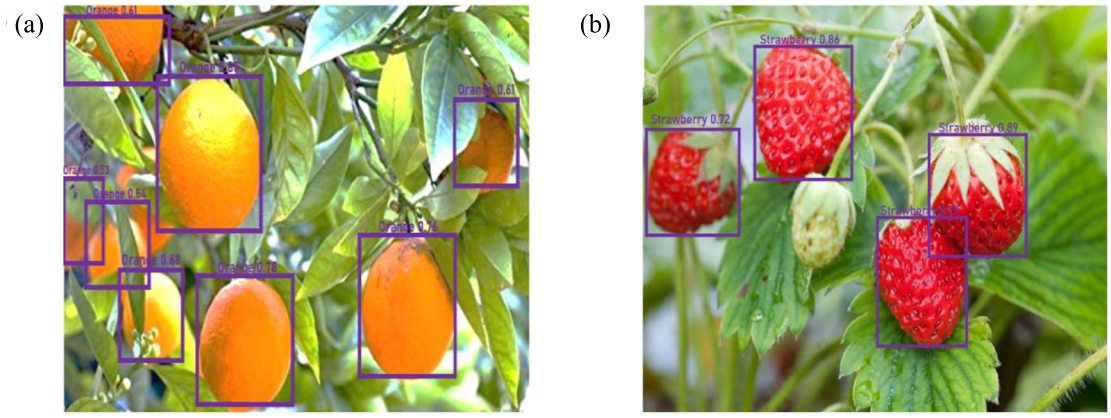

Figure 6. Fruit detection using the fine-tuned CNN model: (a) for oranges, and (b) for strawberries.

Table 2. Hyperparameters for the CNN model.

Hyperparameter	Value
Model Architecture	MobileNetV2 (modified)
Optimizer	Adam
Learning rate	0.01
Batch Size	32
Loss Function	Cross-entropy
Epoch (max)	70

For oranges, the regression coefficient for CNN confidence was −9.67, indicating that each unit increase in confidence significantly reduced the trajectory length, thereby highlighting the model's reliance on accurate fruit detection. The gripper type had a smaller positive coefficient of +0.34, suggesting that different gripper types had a relatively minor but measurable effect on the trajectory. The quadratic orientation deviation term had a coefficient of +0.02, indicating a slight increase in trajectory length when deviating from the optimal 90° orientation. Figure 7 shows the scatter plot for the multi-regression model for oranges. In contrast, the strawberry model yielded a CNN confidence coefficient of −6.41, which also reflected a beneficial effect of improved detection, though less pronounced than for oranges. The gripper type had a coefficient of +0.25, again indicating a modest impact. However, the quadratic orientation term was +0.04, showing a much stronger penalty for misalignment. Figure 8 shows the scatter plot for the multi-regression model for strawberries. This emphasized that strawberries, being more delicate, were more sensitive to orientation errors during the harvesting process. These regression coefficients collectively revealed the relative significance of each factor for different fruit types. CNN confidence consistently emerged as the most influential parameter for minimizing trajectory length in both models. However, orientation accuracy proved to be particularly critical for soft fruits like strawberries due to their higher susceptibility to damage, highlighting the need for precise control during robotic harvesting.

Evaluating the model accuracy is critical for validating the predictive reliability and generalizability of the developed model. Accurate prediction ensures optimal trajectory planning, energy efficiency, and minimal mechanical wear, which are essential in real-time robotic harvesting tasks. The metrics used for evaluation of the model, Coefficient of Determination (R^2), Root Mean Squared Error (RMSE), and Mean Absolute Percentage Error (MAPE), are employed to comprehensively assess the model's performance. The Coefficient of Determination (R^2) quantifies the proportion of variance in the detected trajectory length justified by the regression model. A higher R^2 value (closer to 1) is an indicator of a strong correlation between the actual and predicted values, validating the model's explanatory strength. RMSE endows an absolute measure of prediction error in the same unit as the trajectory length (dependent variable), resulting in a substantial penalty for significant deviations; it is especially sensitive to outliers. By providing a clear grasp of the error magnitude in relation to the actual values, MAPE, mentioned as a percentage, makes it easier to compare data from various datasets or settings. Collectively, these metrics provide a consistent framework for model validation and ensure that the regression model not only fits the training data but also predicts accurately in varying conditions, which is a critical requirement for the deployment of the intelligent and adaptive robotic systems in unstructured agricultural conditions. The subsequent formulas are applied to compute the $R^{2,}$ RMSE, and MAPE:

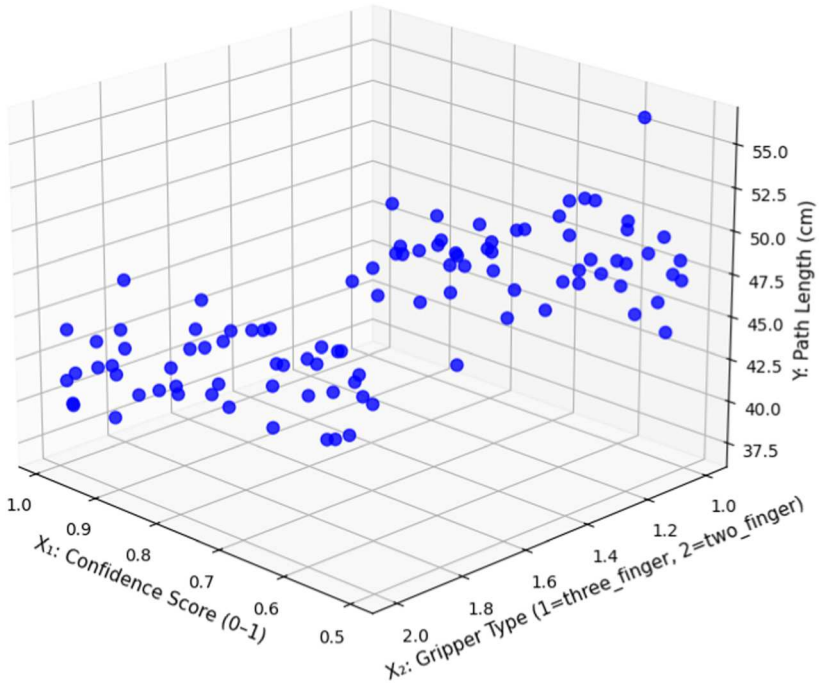

Figure 7. 3D regression scatter plot for orange fruit.

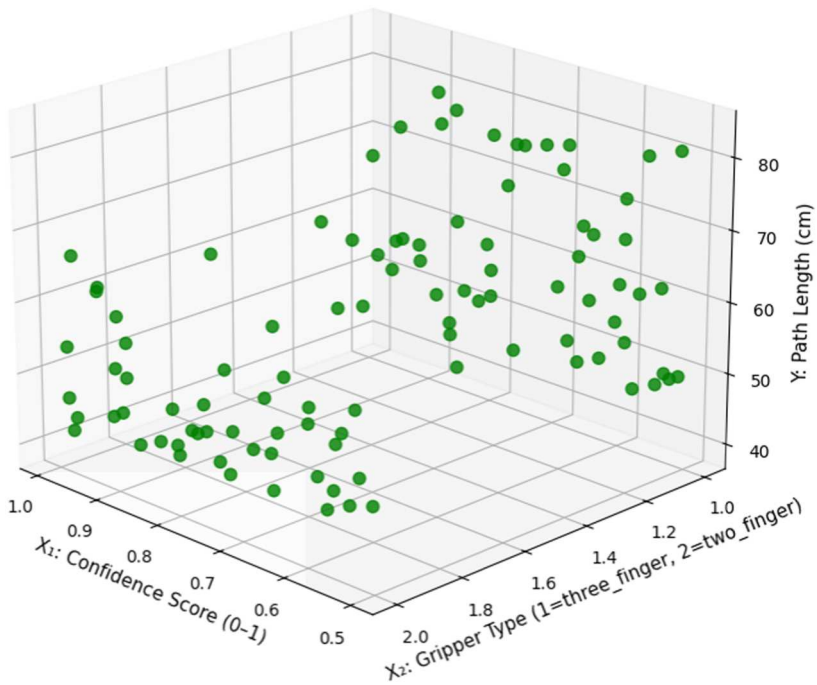

Figure 8. 3D regression scatter plot for strawberry fruit.

$$R^2 = 1 - \sum(TL_{actual} - TL_{predicted})^2 / \sum(TL_{actual} - \bar{TL})^2$$

$$RMSE = \sqrt{1}/n \sum_{i=1}^{n} (TL_{actual} - TL_{predicted})^2$$

$$MAPE = \frac{100}{n} \sum_{i=1}^{n} |(TL_{actual} - TL_{predicted}) / TL_{actual}|$$

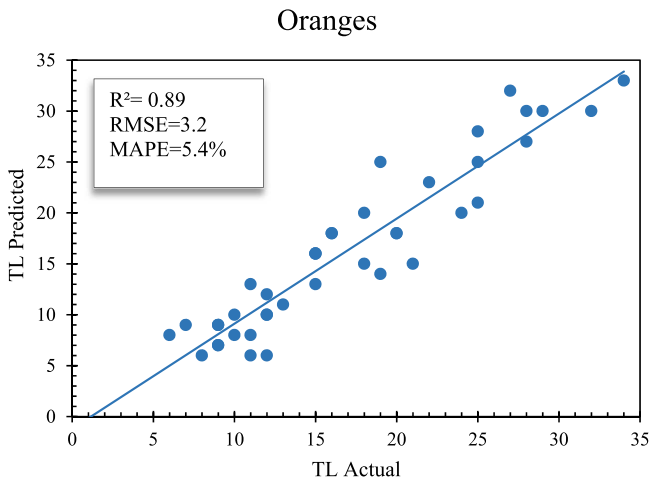

Figure 9. Relationship between actual trajectory planning and predicted trajectory length for oranges.

Where, $\overline{T}$ L is the mean length of the actual trajectory, TL_{actual} is the actual trajectory and $TL_{predicted}$ is the predicted trajectory length, whereas n is the number of test samples and i is the index variable.

To rigorously evaluate the predictive performance of the developed regression models, three well-established statistical metrics were utilized: Coefficient of Determination (R^2), Root Mean Squared Error (RMSE), and Mean Absolute Percentage Error (MAPE). These metrics collectively provide a multidimensional assessment of the models' explanatory capacity, residual behavior, and generalization accuracy. The Coefficient of Determination (R^2) measures the proportion of variance in the dependent variable (trajectory length) that is accounted for by the independent variables in the regression model. R^2 value approaching unity signifies a high degree of correlation between the actual and predicted values. The model for oranges achieved an R^2 of 0.89, signifying that 89% of the variability in trajectory length could be explained by the CNN confidence, gripper type, and orientation deviation parameters. This high R^2 underscores the robustness of the model for firm fruits, which exhibit relatively stable interaction dynamics during robotic handling. By contrast, the strawberry model produced an R^2 of 0.82, indicating a moderate decline in predictive strength. This decrease can be attributed to the higher variance brought about by strawberries' soft texture and geometric irregularity, which intensify the impact of little manipulation and perceptual changes.

The residuals' standard deviation is measured by the RMSE metric. It is therefore sensitive to outliers or inaccurate forecasts and imposes a heavier penalty for larger deviations. With an RMSE of 3.2 cm, the orange model produced predictions that were tightly clustered around the ground truth. The strawberry model, on the other hand, had a larger RMSE of 4.7 cm, which is in line with the high variability that is anticipated when manipulating soft-bodied fruits. For robotic harvesting systems, these RMSE values fall below acceptable operating thresholds, where minor trajectory deviations are tolerable without sacrificing grasp reliability. To facilitate inter-model comparison among datasets of different dimensions, MAPE, which is presented as a percentage, assesses the average magnitude of prediction errors in relation to the actual values. The MAPE was found to be 5.4% for oranges and 7.9% for strawberries. At a performance level of less than 8%, these figures, on average, demonstrate that the models' predictions differed from the observed trajectory lengths. It is in line with agricultural robotics' precision requirements in a semi-structured setting. Strawberries' increased MAPE emphasizes improved control over sensor feedback and end-effector posture while also highlighting their sensitivity to detection and alignment errors. The coefficient of determination (R^2), mean absolute percentage error (MAPE), and root mean square error (RMSE) for the model that forecasts trajectory length during orange harvesting are shown in figure 9. The statistical performance measures for the strawberry harvesting model are also shown in figure 10.

Generally, the higher R^2 values, lower RMSE, and satisfactory MAPE results validate the accuracy of the regression models, along with their operational suitability. Figure 11 displays a comparative analysis of the evaluation metrics, R^2, RMSE, and MAPE, for fruit-specific models developed for orange and strawberry harvesting. These findings confirm that the proposed parameter-driven models are capable of accurately forecasting trajectory length outcomes based on perceptual and mechanical input features. This reliability is important for ensuring accurate trajectory optimization within A^* frameworks, eventually improving spatial efficiency and target achievement rates in autonomous harvesting applications.

The optimized A^* trajectory planning algorithm was implemented in Python with the robot's workspace represented in a grid form. The environment was modeled as a 2D occupancy grid using NumPy arrays. Each cell represented a discrete location marked as either free (0) or occupied (1) based on the presence of obstacles

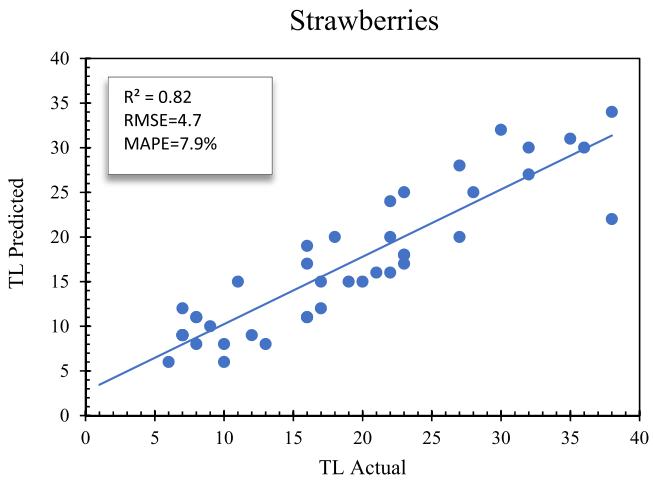

Figure 10. Relationship between actual trajectory planning and predicted trajectory length for strawberries.

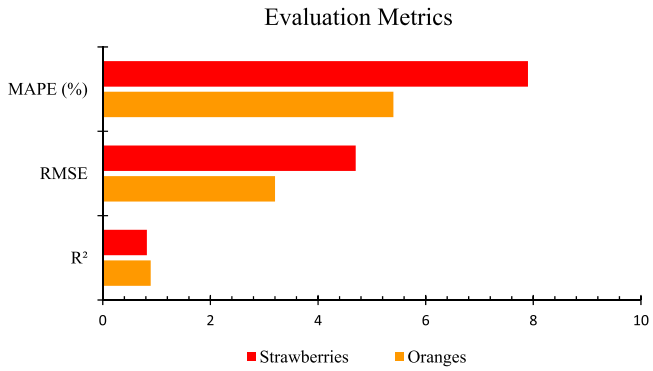

Figure 11. Comparison of regression evaluation metrics for fruit-specific models for oranges and strawberries.

or unreachable zones. The start and goal positions of the robot were defined on the grid coordinates. Each cell in the grid was treated as a node, and movement was allowed in eight directions (including diagonals). A modified cost function was used to integrate three critical parameters, CNN confidence score, gripper angle deviation, and gripper type, into the A* algorithm. These parameters were incorporated into the g(n) term (actual cost) using weighted penalties: low CNN confidence increased the cost; larger angular deviations from the optimal gripper orientation were penalized; and gripper types were assigned static weights based on complexity and suitability for the fruit. The heuristic h(n) was calculated using Euclidean distance from the current node to the goal. A priority queue was managed using Python's heapq module to store the open list sorted by total cost $f(n) = g(n) + h(n)$. Once the optimal trajectory was found, it was reconstructed using a parent dictionary to backtrack from the goal node to the start. The entire planned trajectory was visualized using matplotlib, showing the robot trajectory, fruit locations, and obstacle regions. Figure 12 compares the performance of baseline A* trajectory planning (left) with the proposed optimized A* algorithm (right) for autonomous orange harvesting in a grid-based environment featuring five circular obstacles. In the trajectory plots for the orange orchard, a 5×5 unit grid is used for visualization. Each unit in this grid corresponds to 10 cm in the physical workspace. This scale is selected to reflect the typical inter-tree spacing and maneuvering requirements in orange orchards. The optimized trajectory exhibits a clear improvement, reducing the total number of steps from 40 to 36. This enhancement stems from integrating a regression-based cost function that accounts for three influential factors: CNN detection confidence (X1), gripper type (X2), and gripper orientation angle (X3). The significant negative weight assigned to the confidence score directs the robot to avoid uncertain zones, while the quadratic orientation term encourages gripper alignment closer to 90°, promoting stable and damage-free grasping. Consequently, the optimized A* trajectory not only becomes shorter but also more aligned with mechanical and perceptual constraints, reinforcing the value of coupling machine vision and actuator dynamics in precision agricultural robotics.

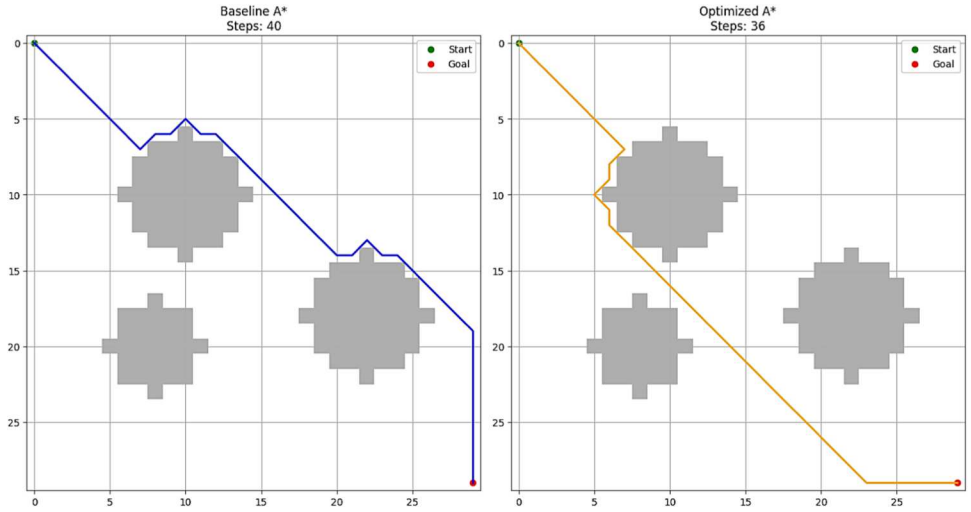

Figure 12. Sample simulation of baseline versus optimized A* trajectory Planning for oranges using a Regression-Informed Cost Function.

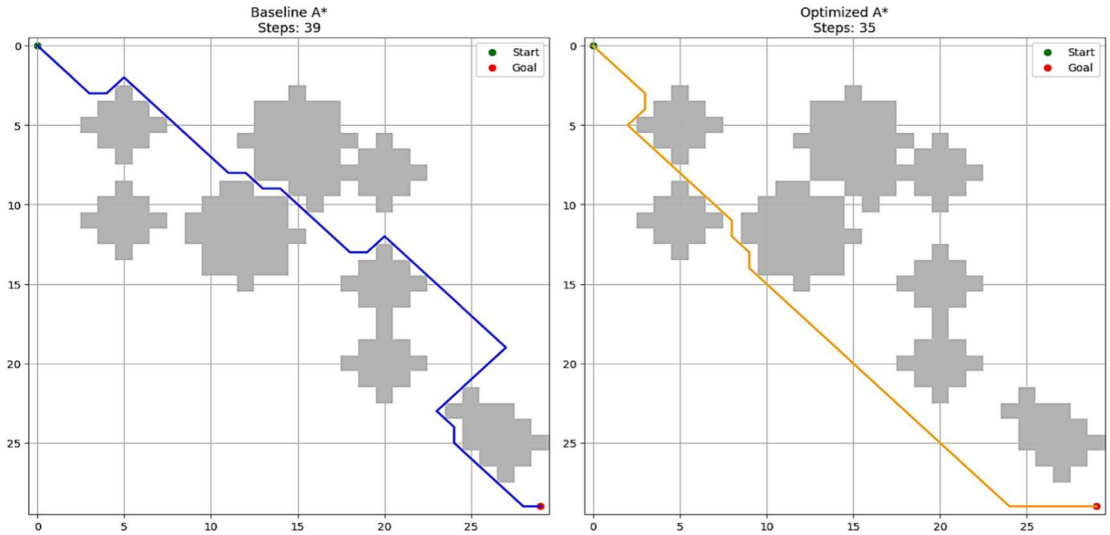

Figure 13. Sample simulation of baseline versus optimized A* trajectory planning for strawberries using Regression-Informed Cost Function.

Figure 13 illustrates a comparative analysis between baseline A* trajectory planning (left) and the proposed regression-informed optimized A* algorithm (right) in a 2D grid environment with five circular obstacles. For the strawberry field scenario, the same 5×5 unit grid is applied, with each unit representing 5 cm of physical space. This finer scale is suitable for representing the denser plant arrangement and supports accurate navigation in narrow inter-row gaps typical of strawberry cultivation. The optimized trajectory demonstrates a reduction in step count from 39 to 35, indicating improved trajectory efficiency. This enhancement results from integrating key perceptual and mechanical parameters, namely, CNN detection confidence, gripper type, and gripper orientation, into the trajectory cost function. The model assigns higher traversal cost to regions of low visual confidence and penalizes gripper misalignment using a symmetric quadratic term, thereby guiding the robot through zones with reliable perception and favorable end-effector alignment. As a result, the optimized trajectory avoids uncertain or mechanically unfavorable regions without compromising safety or goal attainment. This integration of sensory intelligence and actuator constraints enables a more adaptive and operationally efficient navigation strategy, highlighting the effectiveness of data-driven cost modeling in agricultural robotics.

Figure 14 shows the 3D trajectory plot of the sample simulations of another case for a more comprehensive spatial understanding of the robot's movement. The 3D trajectory plot also reveals vertical variations. The plots

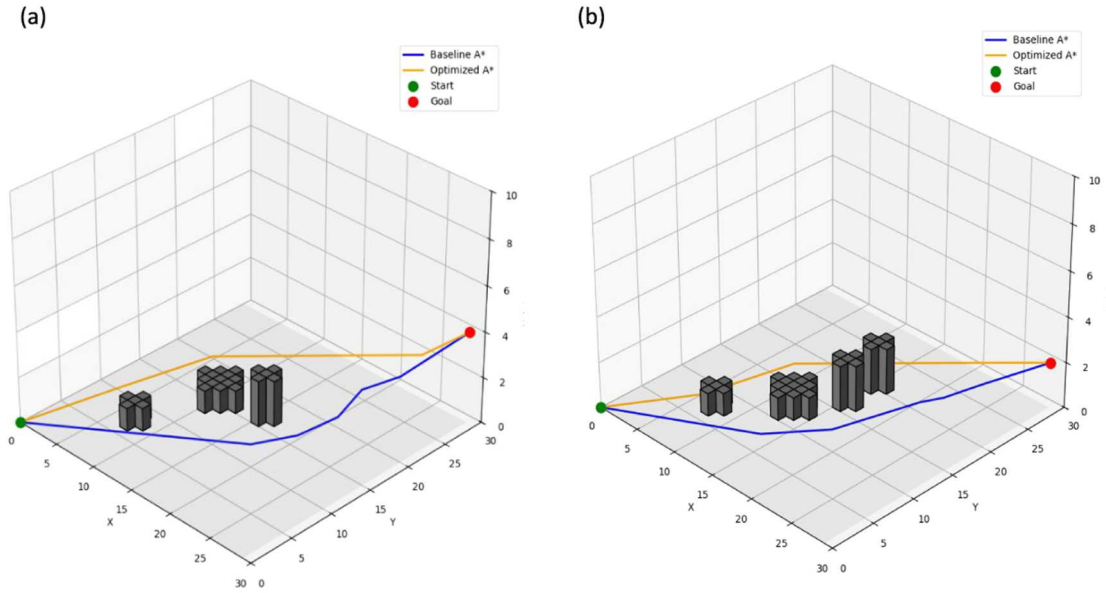

Figure 14. 3D trajectory plots for spatial comparison of baseline and optimized A* paths. (a) oranges case (b) strawberries case.

Table 3. Comparison of trajectory lengths before and after optimization using parameter-driven A* planning.

Fruit type	Baseline trajectory length (cm)	Optimized trajectory length (cm)	Improvement (%)
Oranges	25.58	22	14
Strawberries	31.46	28	11

illustrate the comparison between baseline and optimized trajectories using the A* algorithm for two fruit scenarios: oranges (part a) and strawberries (part b). The baseline trajectory is shown in blue, while the optimized trajectory is in orange. The 3D plots highlight the improvements in movement efficiency and spatial coverage when using optimized A* planning over the baseline trajectory.

To evaluate the effectiveness of the parameter-driven A* planning method, two core performance indicators were analyzed: average trajectory length and positional accuracy at grasping. These metrics directly relate to energy efficiency and successful fruit acquisition. Table 3 presents a comparison of trajectory lengths obtained before and after optimization using the parameter-driven A* planning algorithm. The integration of regression-derived insights into the A* trajectory planning framework significantly enhanced the performance of the robotic harvesting system, as evidenced by a substantial reduction in average trajectory length for both fruit types under investigation. Specifically, the optimized model achieved a 14% decrease in average trajectory length for oranges and an 11% reduction for strawberries relative to the baseline trajectories generated using conventional A* planning without parameter adjustment. Figure 15 shows the trajectory improvements due to optimization. These improvements are indicative of a more informed and adaptive planning process, wherein the regression models provided quantifiable relationships between key input variables, mainly CNN confidence, gripper type, and orientation, along with the expected trajectory length output. By embedding these relationships into the heuristic function and cost evaluation criteria of the A* algorithm, the system was able to generate more efficient and context-sensitive trajectories that inherently minimized unnecessary movement, redundant manoeuvres, and suboptimal grasping approaches. The observed trajectory length reduction is of particular significance in autonomous harvesting operations, where trajectory optimization directly correlates with time efficiency. In robotic systems, shorter and smoother trajectory reduce actuation cycles and wear on joint assemblies, leading to improved operational sustainability. Furthermore, optimized trajectories are more likely to maintain safe distances from obstacles and dynamic elements in unstructured field environments, thereby improving navigation reliability.

In parallel to trajectory improvements, a marked enhancement in positional accuracy was also observed following the integration of the regression-informed planning strategy. Table 4 presents a comparison of positional accuracy obtained before and after optimization using the parameter-driven A* planning algorithm. The accuracy of end-effector positioning at the fruit location increased by 10% for oranges and 12% for strawberries. Figure 16 shows the improvements in positional accuracy due to optimization. This improvement can be

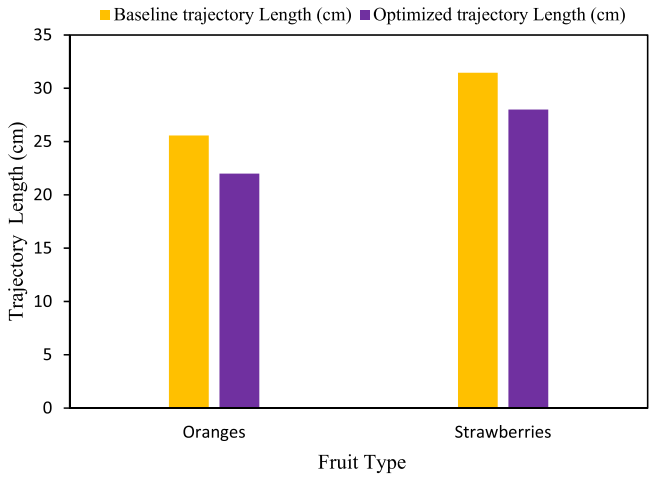

Figure 15. Trajectory length reduction through parameter-driven A* optimization.

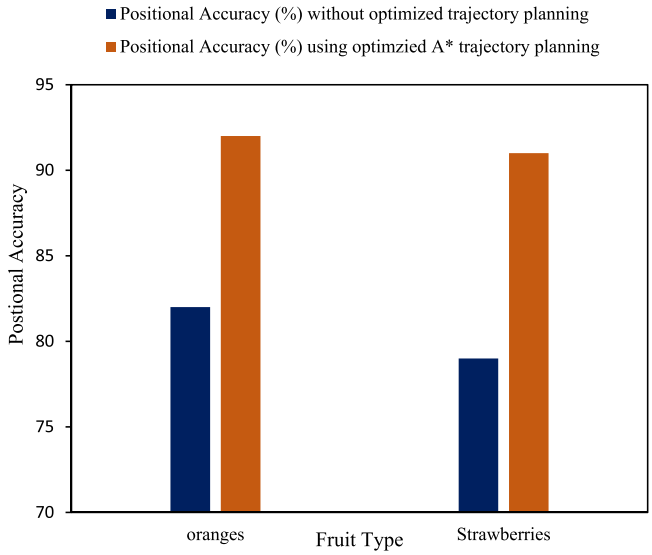

Figure 16. Improvement in positional accuracy through parameter-driven A* trajectory planning.

Table 4. Comparison of positional accuracy before and after A* optimization.

Fruit type	Positional accuracy (%) without optimized trajectory planning	Positional accuracy (%) using optimized A* trajectory planning	Improvement (%)
Oranges	82	92	12
Strawberries	79	91	15

attributed to the reduced variability in gripper alignment and motion execution, as the planner increasingly favoured configurations that aligned with statistically optimal conditions derived from the regression model. The effect is particularly pronounced for strawberries, which are more sensitive to mechanical misalignment due to their soft texture and susceptibility to bruising. Enhanced positional accuracy minimizes the probability of partial grasps or contact-induced damage, which are critical concerns in maintaining post-harvest quality and ensuring successful pick-and-place operations.

Real-time trajectory planning was conducted on a system equipped with a Core i7 processor (2.30 GHz), 16 GB RAM, and a GPU with 6 GB VRAM. The vision module achieved an average inference speed of 20 frames per second (FPS), while local trajectory planning was completed within 0.7 s per cycle across all test cases. These computational specifications enabled seamless integration of CNN-based fruit detection, grasp point

estimation, and dynamic trajectory optimization without processing bottlenecks, thereby supporting real-time operation in both greenhouse and orchard environments. These results indicate that real-time operation can be maintained without requiring high-end infrastructure. Consequently, the computational time does not impose a significant burden on production costs. Therefore, under monotype conditions, the overall cost of production remains manageable, supporting the practical feasibility of commercial deployment.

These findings underscore the synergistic benefits of coupling data-driven modeling with classical search-based planning algorithms. The regression model not only served as a predictor of trajectory length outcomes but also functioned as a feedback mechanism that refined the planner's behavior in real-time. This integration facilitated a higher degree of cohesion between the perception system (CNN-based fruit detection), the manipulation subsystem (gripper configuration and orientation), and the motion planning logic (A^* trajectory generation). Such alignment is fundamental for effective performance in complex agricultural environments, where variability in fruit position, occlusion, terrain, and lighting conditions necessitate adaptive and intelligent behavior from autonomous platforms. Hence, the incorporation of multivariate regression outputs into the A^* framework led to demonstrable gains in both spatial efficiency and targeting accuracy. These enhancements validate the utility of parameter-driven trajectory planning and suggest a promising direction for the development of intelligent agricultural robots capable of real-time adaptation and optimization. Future extensions could include the use of dynamic regression models trained under varying environmental contexts or the embedding of real-time learning components to enable continual refinement of the planning strategy during field deployment. Despite the promising outcomes, certain limitations must be acknowledged. The current study only evaluates two types of grippers, three-finger and two-finger designs, which are widely adopted due to their established effectiveness. However, future studies should explore a broader array of end-effectors, including suction-based and scissor-type grippers, to provide a more comprehensive understanding of gripper-specific interactions with trajectory planning. The study also focuses exclusively on the A^* algorithm. Comparative analyses involving alternative trajectory planning strategies, such as Dijkstra (D^*), Rapidly exploring Random Tree (RRT^*), or learning-based methods, would provide valuable insights into the relative performance and adaptability of each approach. Additionally, the scope of the study is limited to only two fruit types. Incorporating a wider range of fruits with varying shapes, sizes, and fragilities would improve the models' generalizability and allow their application across more diverse harvesting scenarios. The results of this regression-guided A^* trajectory planning framework show the effectiveness of integrating statistical modeling into autonomous robotic systems. The current study quantifies the impact of manipulation and perception parameters on motion efficiency and develops adaptive and data-driven harvesters proficient in working under different agricultural environments. By adaptively adjusting its cost function with contextual data, reinforcement learning can improve the A^* for future work, leading to more effective pathways and better obstacle avoidance in dynamic harvesting scenarios. Moreover, the color dependence may limit its success for detecting green fruits, such as pears, where low background contrast poses a prospective challenge. However, the future work needs to focus on adding depth cues and shape-based features during model training. To increase detection robustness over a larger variety of fruit species, multispectral imaging is also advised.

Conclusions

- The trajectory planning is a key factor in autonomous robotic harvesting systems as it directly affects operating efficiency, energy consumption, collision avoidance, and fruit acquisition success. The conventional geometry-based planning methods limit the flexibility in responding to real-time sensory data and mechanical constraints during unstructured agricultural settings, where fruit types and orientation undergo frequent variations.
- Through perception-informed and actuator-aware motion optimization, the current study highlights the need to combine data-driven regression modeling with traditional A^* trajectory planning to enhance robotic fruit harvesting performance.
- The average trajectory length is reduced by 14% for oranges and 11% for strawberries when multivariate regression results are used, indicating a quantifiable increase in trajectory planning efficiency.
- CNN detection confidence is the dominant predictor among the modeled variables, demonstrating how critical precise fruit localization is for maximizing navigation and minimizing redundancy in planned motion.
- The system can penalize misalignment symmetrically by incorporating a quadratic orientation term, which is especially helpful when handling soft fruits like strawberries, where end-effector alignment is essential to preventing damage.

- The regression models exhibited strong predictive capability, achieving R^2 values of 0.89 and 0.82, with RMSE of 3.2 cm and 4.7 cm, and MAPE of 5.4% and 7.9%, respectively, for oranges and strawberries.
- Positional accuracy during fruit grasping improved by 12% for oranges and 15% for strawberries, indicating enhanced coordination between visual perception, motion planning, and mechanical execution.
- The results validate the potential of coupling sensory data, gripper dynamics, and trajectory planning in a unified framework to achieve more intelligent and responsive robotic behavior in unstructured agricultural settings.
- Future work should focus on expanding the approach to incorporate a wider range of fruit types, diverse gripper architectures, and comparative evaluations with alternative planning algorithms for broader applicability and real-time field deployment. Furthermore, incorporating depth cues and shape-based features into model training is recommended to improve detection robustness. Moreover, reinforcement learning can be integrated with A^* by adaptively tuning its cost function parameters based on environment feedback to optimize path efficiency and obstacle avoidance.

Acknowledgments

The authors gratefully acknowledge the University of Central Punjab, University of Technology Sydney, and University of Engineering and Technology, Lahore, for their guidance and technical support.

Conflict of interest

The authors declare no conflict of interest.

Data availability statement

The data contains proprietary experimental recordings and image data collected under collaborative agreements with our industry partner and is to be used for further research projects. However the data can be made available upon reasonable request. The data that support the findings of this study are available upon reasonable request from the authors.

Author contributions

Sadaf Zeeshan 0000-0003-2776-9031
Conceptualization (equal), Data curation (equal), Formal analysis (equal), Investigation (equal), Writing – original draft (equal), Writing – review & editing (equal)

Muhammad Ali Ijaz Malik 0000-0002-0227-4289
Data curation (equal), Formal analysis (equal), Investigation (equal), Methodology (equal), Writing – original draft (equal)

Tauseef Aized
Project administration (equal), Supervision (equal), Validation (equal), Visualization (equal), Writing – review & editing (equal)

Akbar Ali
Investigation (equal), Methodology (equal), Software (equal)

Simran Ejaz
Investigation (equal), Software (equal), Validation (equal), Writing – original draft (equal)

Faiza Javaid 0009-0004-3994-7901
Data curation (equal), Formal analysis (equal), Investigation (equal), Methodology (equal)

References

[1] Sukanya M and Avijit G 2024 Agriculture paradigm shift: a journey from traditional to modern agriculture *Biodiversity and Bioeconomy* 113–41
[2] Christiaensen L, Rutledge Z and Taylor J E 2021 The future of work in agri-food *Food Policy* **vol. 99** 101963
[3] 2025 https://data.worldbank.org/indicator/FP.CPI.TOTL.ZG
[4] Razzaq A 2025 Why young pakistanis are leaving farming *Agricultural Economics* https://amarrazzaq.com/insights/why-young-pakistanis-leaving-farming.html?
[5] 2025 Pakistan Economy Dashboard *Pakistan Economic Survey* https://www.finance.gov.pk/survey_2025.html
[6] 2025 Farmonaut *7 Economic Impacts* https://farmonaut.com/precision-farming/autonomous-robots-in-agriculture-7-economic-impacts-2025
[7] Marcelo Rodrigues B J, Regimar Garcia dos S, Lucas de Azevedo S and Luan Pereira de O 2024 Advancements in agricultural ground robots for specialty crops: an overview of innovations, challenges, and prospects *Plants* **13** 3372
[8] Jun Z, Ningbo K, Qianjin Q, Lianghuan Z and Hongbo Z 2024 Automatic fruit picking technology: a comprehensive review of research advances *Artif. Intell. Rev.* **57** 54
[9] Maria H, Shruti P and Christof B 2024 Optimal guidance track generation for precision agriculture: a review of coverage path planning techniques *J. Field Rob.* **41** 823–44
[10] Vishnu R, Bappaditya D, Sariah M, Willow M, Soran P, Simon P and Amir G-E 2023 Towards autonomous selective harvesting: a review of robot perception, robot design, motion planning and control *J. Field Rob.* **41** 2247–79
[11] Tantan J and Xiongzhe H 2024 Robotic arms in precision agriculture: a comprehensive review of the technologies, applications, challenges, and future prospects *Comput. Electron. Agric.* 108938
[12] Wei Z, Ning G, Baohua Z, Jun Z, Guangzhao T and Yingjun X 2022 Human grasp mechanism understanding, human-inspired grasp control and robotic grasping planning for agricultural robots *Sensors* **22** 5240
[13] Paula P, Bettina L, Ana Inés M, Esteban V and Joanna L 2024 Exploration of strawberry fruit quality during harvest season under a semi-forcing culture with plants nursed without chilling *Plants* **13** 3052
[14] Sania H, Kanchan S, Kewal K and Ankita T 2024 Types and cultivation of citrus fruits *in Citrus Fruits and Juice Singapore* (Springer)
[15] Luis T, Akram G, Zixuan H, Yunjun X, Manoj K and Reza E 2024 A small autonomous field robot for strawberry harvesting *Smart Agricultural Technology* **8** 100454
[16] Yang Y, Hehe X, Kailiang Z, Yujie W, Yutong L, Jianmei Z and Lizhang X 2024 Design, development, integration, and field evaluation of a ridge-planting strawberry harvesting robot *Agriculture* **14** 2126
[17] Hehe X, Dongxing Z, Li Y, Tao C, Xiantao H, Kailiang Z and Zhijie Z 2024 Development, integration, and field evaluation of a dual-arm ridge cultivation strawberry autonomous harvesting robot *J. Field Rob.* **42** 1783–98
[18] Zixuan H, Zibo L, Zhiyan Z, Manoj K and Qin Z 2025 Improving picking efficiency under occlusion: design, development, and field evaluation of an innovative robotic strawberry harvester *Comput. Electron. Agric.* **237** 110684
[19] Hesheng Y *et al* 2023 Development, integration, and field evaluation of an autonomous citrus-harvesting robot *J. Field Rob.* **40** 101343
[20] Sadaf Z, Tauseef A and Fahid R 2024 In-depth evaluation of automated fruit harvesting in unstructured environment for improved robot design *Machines* **12** 151
[21] Xu X, Yaonan W, Bing Z and Yiming J 2024 Flexible hand claw picking method for citrus-picking robot based on target fruit recognition *Agriculture* **14** 1227
[22] Feng X, Haibin W, Yueqin X and Ruiqing Z 2023 Fruit detection and recognition based on deep learning for automatic harvesting: an overview and review *Agronomy* **13** 1625
[23] Sadaf Z, Tauseef A and Fahid R 2023 The design and evaluation of an orange-fruit detection model in a dynamic environment using a convolutional neural network *Sustainability* **15** 4329
[24] Nithya R *et al* 2022 Computer vision system for mango fruit defect detection using deep convolutional neural network *Foods* **11** 3483
[25] Sinan U, Gulhan Ş and Abdullah Y 2023 Disease detection and physical disorders classification for citrus fruit images using convolutional neural network *Journal of Food Measurement and Characterization* **17** 2353–62
[26] EungChan K, Suk-Ju H, Sang-Yeon K, Chang-Hyup L, Sungjay K, Hyuck-Joo K and Ghiseok K 2022 CNN-based object detection and growth estimation of plum fruit (Prunus mume) using RGB and depth imaging techniques *Sci. Rep.* **12** 20796
[27] Ramazan H-R, Ezzatollah Askari A-A, Ahmad J, Esmaili -A I and Sajad S 2023 Intelligent detection of citrus fruit pests using machine vision system and convolutional neural network through transfer learning technique *Comput. Biol. Med.* **155** 106611
[28] Anand U, Sunny S and Shona K 2023 Segregation of ripe and raw bananas using convolutional neural network *Procedia Computer Science* **218** 461–8
[29] O *et al* 2024 Convolutional neural network ensemble learning for hyperspectral imaging-based blackberry fruit ripeness detection in uncontrolled farm environment *Eng. Appl. Artif. Intell.* **132** 107945
[30] Jifei Z *et al* 2024 YOLO-granada: a lightweight attentioned yolo for pomegranates fruit detection *Sci. Rep.* **14** 16848
[31] Rongli G, Na C and Hai Y 2021 A detection algorithm for cherry fruits based on the improved YOLO-v4 model *Neural Computing and Applications* **35** 13895–906
[32] Aljaafreh A, Ezzaldeen Y E, Jafar A, Abdel-Hamid S, Saqer S. A A, Aparajithan S and James H 2023 A real-time olive fruit harvesting robot based on yolo algorithms *Acta Technologica Agriculturae* **3** 121–32
[33] Yishen L, Zifan H, Yun L, Yunfan L and Weipeng J 2024 AG-YOLO: a rapid citrus fruit detection algorithm with global context fusion *Agriculture* **14** 114
[34] Lawal O M 2023 Real-time cucurbit fruit detection in greenhouse using improved YOLO series algorithm *Precision Agriculture* **25** 347–59
[35] Yan W, Gang Y, Qinglu M, Ting Y, Jianfeng H and Bo Z 2022 DSE-YOLO: detail semantics enhancement YOLO for multi-stage strawberry detection *Comput. Electron. Agric.* **198** 107057
[36] Yongpeng X, Mingming L, Qian X and Ruting X 2024 Design and analysis of a robotic gripper mechanism for fruit picking *Actuators* **13** 338
[37] Junchang Z, Rongrong Z, Yucai S, Na L, Qing W and Haotun L 2025 Force sensing and force control of flexible gripper with integrated flexible strain and tactile sensors for strawberry non-destructive gripping and freshness grading *Food Bioprocess Technol.* **18** 5700–21
[38] Eleni V, Viktoria Nikoleta T, Ioannis K, Theodoros G, Theodore P, Vassilis K and G 2022 An overview of end effectors in agricultural robotic harvesting systems *Agriculture* **12** 1240
[39] Christopher L, Andrew E, Christopher M, Adam T, W and Tristan P 2017 Autonomous sweet pepper harvesting for protected cropping systems *IEEE Robotics and Automation Letters* **2** 872–9

[40] Linlu Z, Yanping Z, Jiuqin L, Fei S, Yan Z and Pingzeng L 2021 Detection and segmentation of mature green tomatoes based on mask r-cnn with automatic image acquisition approach *Sensors* **21** 7842
[41] Inkyu S, Zongyuan G, Feras D, Ben U, Tristan P and Chris M 2016 DeepFruits: a fruit detection system using deep neural networks *Sensors* **16** 1222
[42] Wang F 2023 ABC: adaptive, biomimetic, configurable robots for smart farms-from cereal phenotyping to soft fruit harvesting,' University of Essex
[43] Bai Y, Guo Y, Zhang Q, Cao B and Zhang B 2022 Multi-network fusion algorithm with transfer learning for green cucumber segmentation and recognition under complex natural environment *Comput. Electron. Agric.* **194** 106789
[44] Roggiolani G, Bailey B N, Behley J and Stachniss C 2025 Generation of labeled leaf point cloudsfor plants trait estimation *Plant Phenomics* 100071
[45] Singh R, Seneviratne L and Hussain I 2024 A deep learning-based approach to strawberry grasping using a telescopic-link differential drive mobile robot in ros-gazebo for greenhouse digital twin environments *IEEE Access* **13** 361–81
[46] Zhang Y, Li L, Chun C, Wen Y, Li C and Xu G 2024 Data-driven bayesian gaussian mixture optimized anchor box model for accurate and efficient detection of green citrus *Comput. Electron. Agric.* **225** 109366
[47] Kaleem A, Hussain S, Aqib M, Cheema M J M, Saleem S R and Farooq U 2023 Development challenges of fruit-harvesting robotic arms: a critical review *AgriEngineering* **5** 2216–37
[48] Miao Z *et al* 2023 Efficient tomato harvesting robot based on image processing and deep learning *Precision Agriculture* **24** 254–87
[49] Eduardo N, Roemi F, Delia S, Manuel A and Pablo G-d-S 2021 Soft grippers for automatic crop harvesting: a review *Sensors* **21** 2689
[50] E, Johannes F, Dimitra D, Della S C and Abdel-Hamid S 2022 Soft robotic grippers for crop handling or harvesting: a review *IEEE Access* **10** 75428–43
[51] Francesco V, Fabio C and Riccardo M 2023 A soft, sensorized gripper for delicate harvesting of small fruits *Comput. Electron. Agric.* **213** 108202
[52] Polina K and Stephanie L 2023 RGB-D datasets for robotic perception in site-specific agricultural operations—a survey *Comput. Electron. Agric.* **212** 108035
[53] Jing Z, Manoj K, Qin Z, Xin Z, Majeed Y, Longsheng F and Shumao W 2020 Multi-class object detection using faster R-CNN and estimation of shaking locations for automated shake-and-catch apple harvesting *Comput. Electron. Agric.* **173** 105384